






## Article

# Muscle Synergy of the Periarticularis Shoulder Muscles during a Wheelchair Propulsion Motion for Wheelchair Basketball

Yuki Tamura <sup>1</sup>, Noriaki Maeda <sup>1,\*</sup>, Makoto Komiya <sup>2</sup>, Yoshitaka Iwamoto <sup>3</sup>, Tsubasa Tashiro <sup>1</sup>, Satoshi Arima <sup>1</sup>, Shogo Tsutsumi <sup>4</sup>, Rami Mizuta <sup>1</sup> and Yukio Urabe <sup>1</sup>

- <sup>1</sup> Graduate School of Biomedical and Health Sciences, Hiroshima University, 1-2-3, Kasumi, Minami-ku, Hiroshima 734-8553, Japan; yuki-tamura@hiroshima-u.ac.jp (Y.T.); tsubasatashiro716@hiroshima-u.ac.jp (T.T.); satoshi-arima4646@hiroshima-u.ac.jp (S.A.); rami-mizuta@hiroshima-u.ac.jp (R.M.); yurabe@hiroshima-u.ac.jp (Y.U.)
- <sup>2</sup> Institute for Human Movement and Medical Sciences, Niigata University of Health and Welfare, 1398, Shimami-cho, Kita-ku, Niigata 950-3102, Japan; makoto-komiya@nuhw.ac.jp
- <sup>3</sup> Division of Rehabilitation, Department of Clinical Practice and Support, Hiroshima University Hospital, 1-2-3, Kasumi, Minami-ku, Hiroshima 734-8553, Japan; iwamo10@hiroshima-u.ac.jp
- <sup>4</sup> Department of Orthopedic Surgery, Graduate School of Medical and Dental Sciences, Kagoshima University, 8-35-1, Sakuragaoka, Kagoshima 890-8544, Japan; k2711488@kadai.jp
- \* Correspondence: norimmi@hiroshima-u.ac.jp

**Abstract:** Wheelchair basketball players often develop shoulder pain due to repetitive wheelchair propulsion motion. Wheelchair propulsion involves two phases, push and recovery, with several different muscles simultaneously active in each phase. Although differences in the coordinated activity of multiple muscles may influence the mechanism of injury occurrence, there have been no studies investigating muscle synergy in wheelchair propulsion motion. Twelve healthy adult males with no previous wheelchair driving experience were included. The surface electromyography data of 10 muscles involved in shoulder joint movements were measured during a 20 m wheelchair propulsion motion. Muscle synergies were extracted using non-negative matrix factorization analysis of the electromyography data. Four muscle synergies were identified during wheelchair propulsion. Synergy 1 reflects propulsion through shoulder flexion and elbow flexion, while Synergy 2 involves shoulder flexion and elbow extension. Synergy 3 describes shoulder extension returning the upper limb, which has moved forward during the push, back to its original position, and Synergy 4 relates to stabilize the shoulder girdle during the recovery phase. This study is the first to explore muscle synergy during wheelchair propulsion, and the data from healthy participants without disabilities or pain will provide a baseline for future comparisons with data from wheelchair basketball players.

**Keywords:** muscle synergy; wheelchair propulsion motion; shoulder muscles; wheelchair basketball; electromyography; non-negative matrix factorization analysis



**Citation:** Tamura, Y.; Maeda, N.; Komiya, M.; Iwamoto, Y.; Tashiro, T.; Arima, S.; Tsutsumi, S.; Mizuta, R.; Urabe, Y. Muscle Synergy of the Periarticularis Shoulder Muscles during a Wheelchair Propulsion Motion for Wheelchair Basketball. *Appl. Sci.* **2024**, *14*, 9292. <https://doi.org/10.3390/app14209292>

Academic Editors: Ruperto Menayo Antúnez and Juan Pedro Fuentes García

Received: 25 September 2024

Revised: 9 October 2024

Accepted: 10 October 2024

Published: 12 October 2024



**Copyright:** © 2024 by the authors. Licensee MDPI, Basel, Switzerland. This article is an open access article distributed under the terms and conditions of the Creative Commons Attribution (CC BY) license (<https://creativecommons.org/licenses/by/4.0/>).

## 1. Introduction

Wheelchair basketball (WB) is a parasport designed to allow individuals with impaired motor functions to enjoy playing basketball. Although the size of the court and the height of the baskets remain the same as those in basketball, in WB, the game is played while seated in a wheelchair. WB has been an official sport since the first Paralympic Games and is considered one of the most popular sports [1]. Participation in WB provides athletes with several physical and psychological benefits, such as enhanced cardiopulmonary function and muscle strength [2], but also carries a high risk of injury. The Rio 2016 Paralympic Games injury survey reported a high injury incidence rate for wheelchair sports (WB, wheelchair fencing, and wheelchair rugby), with WB having the highest injury incidence rate at 8.0%, compared to wheelchair fencing at 3.1% and wheelchair rugby at 3.9% [3]. Focusing on the site of injuries, injuries to the upper limbs account for 47.2% of all injuries

in WB, with the shoulder joint specifically representing the largest percentage at 22.2% [4]. Athletes participating in WB perform repeated overhead movements, which increases their risk of developing shoulder joint injuries involving the rotator cuff and labrum, compared to other wheelchair sports [5,6]. In fact, between 14.0% and 75.0% of WB players report experiencing shoulder pain, suggesting a significant tendency for shoulder joint injuries among these athletes [7].

In WB, repetitive upper limb movements, such as passing, shooting, and wheelchair propulsion, contribute to the increased incidence of shoulder joint injuries [8]. Particularly, the wheelchair propulsion motion is crucial for achieving better performance in WB, which requires quick movement around the court in a wheelchair [9]. Generally, wheelchair propulsion motion is divided into two phases: the push phase (PP), during which the hands are in contact with the hand rim, and the recovery phase (RP), during which the hands leave the hand rim and last until the hands contact the hand rim again [10]. A study investigating muscle activity during daily wheelchair propulsion reported increased muscle activity of the anterior deltoid (AD), biceps brachii (BB), and pectoralis major (PM) during the PP but increased muscle activity of the middle deltoid (MD), posterior deltoid (PD), and upper trapezius (UT) during the RP [11]. Additionally, the infraspinatus (IS) was active in both the PP and RP phases, and the triceps brachii (TB) began to be active in the latter half of the PP and showed high activity in the RP [11]. Thus, the muscles with high activity in each phase of the propulsion motion differ, with shoulder flexors mainly active in the PP and shoulder extensors mainly active in the RP. However, previous studies have focused only on examining the activity of individual muscles, and there have been no investigations into the coordinated activity of muscles acting simultaneously.

Coordinated muscle activity can be assessed through muscle synergy analysis, which evaluates the functional modules of motion by the central nervous system [12]. Since the modules coordinate the activation of muscle groups with different weights under the control of the nervous system during the accomplishment of certain movements [13], understanding the functional modules in movement can provide insight into basic motor control science and motor coordination strategies [14]. In most cases, the muscle synergies are extracted using the non-negative matrix factorization (NMF) analysis, an algorithm proposed by Lee and Seung [15]. From the electromyography (EMG) data, NMF analysis can be used to extract two components of the module: “muscle weighting”, which indicates the coordination of multiple muscles (muscle synergies), and “activation coefficient”, which determines the timing of the muscle synergy activity. For example, it was found that while the same number of muscle synergies were controlled in the jump landing of chronic ankle instability patients as in healthy participants, the synergies that control knee joint motion by the vastus lateralis and the lateral head of the gastrocnemius were deficient and a compensatory movement strategy by the gluteus maximus was used [16]. In addition, the module of ankle motion showed an increase in the muscle weighting of the tibialis anterior [16]. This was the basis for the demand for a new rehabilitation treatment for patients with chronic ankle instability. Recently, muscle synergy analysis has been applied to sports motion, and muscle synergies differ depending on performance level and the presence of injury [17,18]. Given the expected increase in the number of WB players, the need for studies on performance improvement and injury prevention in WB will likely become even more pronounced. As one measure, understanding the muscle synergy comprising wheelchair propulsion enables the assessment of coordinated muscle activity during movement, leading to more specific and efficient training and injury prevention programs.

In this study, we aimed to investigate the muscle synergy in the periarticularis muscles of the shoulder joint during WB wheelchair propulsion motion. We hypothesized that there are distinct muscle synergies for the PP and RP of wheelchair propulsion motion, with the PP constituting a synergy primarily with the shoulder flexor muscles and the RP constituting a synergy primarily with the shoulder extensor muscles. As a first attempt in this research project, the identification of muscle synergy during wheelchair propulsion motion

in healthy participants unaffected by disability or pain will provide useful information as standard data to be compared with that of wheelchair basketball players in the future.

## 2. Materials and Methods

### 2.1. Participants

Twelve healthy adult males (age,  $23.3 \pm 1.5$  years old; body mass index,  $22.7 \pm 2.7$  kg/m<sup>2</sup>; mean  $\pm$  standard deviation) participated in this study. The inclusion criteria were as follows: (1) no orthopedic disease in the upper limbs, lower limbs, or trunk within the past 6 months, (2) no physical pain at the time of measurement, and (3) no previous experience driving a wheelchair for WB. In this study, healthy participants without any prior experience driving a wheelchair were chosen to eliminate the influence of competition level on muscle synergy. The exclusion and discontinuation criteria included difficulty in continuing measurements due to pain during the measurement. All the participants were right-handed.

Following the principles of the Declaration of Helsinki, the outline of this study was fully explained, and written informed consent was obtained from all the participants. This study was approved by the Ethics Committee for Epidemiology of Hiroshima University (approval number: E2022-0075).

### 2.2. Experimental Setup

The task movement was wheelchair propulsion for 20 m in a straight line with maximum effort. The crossing times at 5 m from the start line and 20 m from the finish line were measured using a stopwatch. Approximately 10 min of practice time was provided to standardize the wheelchair propulsion motion before measurement.

The same WB wheelchair was used for all participants in this study. Therefore, the seat height was adjusted with a cushion such that the elbow joint flexion angle was 100°–120° when grasping the top edge of the hand rim to eliminate the influence of differences in body size among participants [19].

A DSP wireless dry-type myoelectric sensor (SS-EMGD-HMAG; Sports Sensing Corporation, Fukuoka, Japan) with a built-in three-axis acceleration/angular velocity sensor was used to measure the acceleration data during wheelchair propulsion. The sensor was installed behind the wheelchair parallel to the floor. The sampling frequency was 1000 Hz.

Surface EMG was performed using the same electrodes used to measure the acceleration. Because the assumption of bilateral symmetry is considered valid for wheelchair propulsion motion in healthy participants without upper limb pain or disability [20], this study measured muscle activity only on the dominant side. As shown in Figure 1, the electrodes were attached to a total of 10 muscles: latissimus dorsi (LD), AD, MD, PD, BB, TB, IS, PM, UT, and serratus anterior (SA) [11]. The electrode placements were based on previous studies [21,22]. Before attaching the electrodes, the skin was rubbed with alcohol cotton to reduce impedance. Acceleration and surface EMG data were synchronized by unifying the sampling frequency of the electrodes at 1000 Hz.

### 2.3. Data Analyses

All data analyses were performed using the MATLAB numerical analysis software (MATLAB R2023a; MathWorks, Inc., Natick, MA, USA).

The propulsion phase was identified based on the acceleration data in the forward and backward directions. The acceleration data were low-pass filtered at a cutoff frequency of 12 Hz using a fourth-order zero-lag Butterworth filter to remove random noise [23]. In addition, low-pass filtering was applied at a cutoff frequency of 4 Hz to identify the propulsion phase [24]. The point in time when the acceleration transitions from negative to positive values indicates the start of the PP, whereas from positive to negative values indicates the start of the RP (Figure 2). In this study, 10 consecutive propulsion cycle data points from the propulsion motion after passing through the 5 m point were extracted for analysis. The proportion of time that the PP occupied each cycle was calculated, and an average of 10 cycles was obtained.

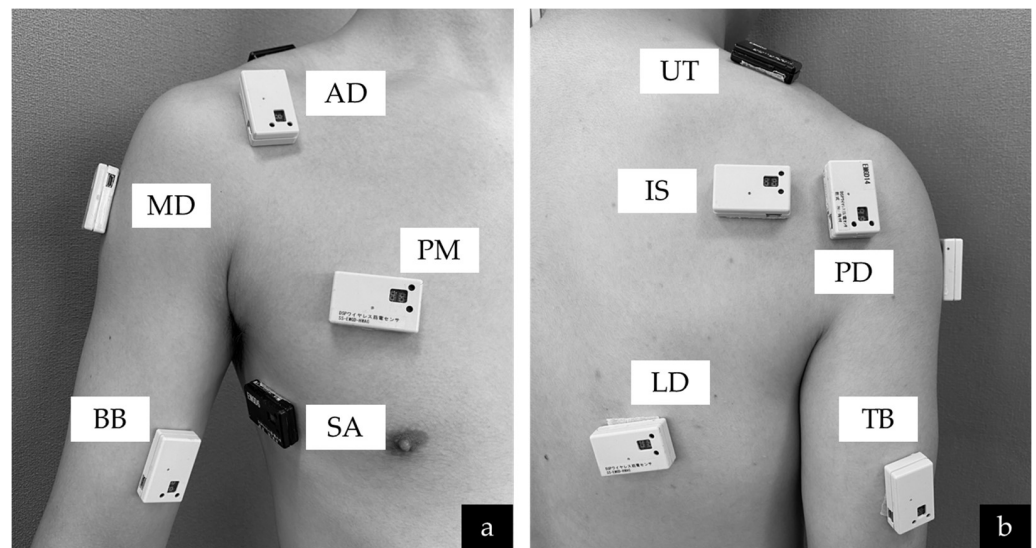


**Figure 1.** Electrode placements. (a) shows the anterior and (b) shows the posterior of the trunk. LD: latissimus dorsi, AD: anterior deltoid, MD: middle deltoid, PD: posterior deltoid, BB: biceps brachii, TB: triceps brachii, IS: infraspinatus, PM: pectoralis major, UT: upper trapezius, SA: serratus anterior.

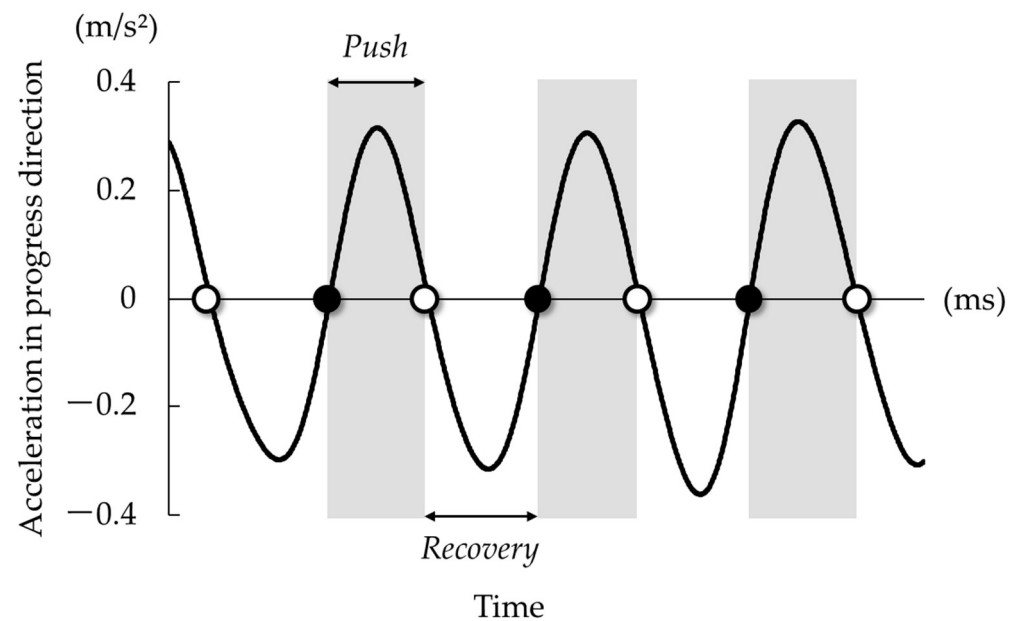


**Figure 2.** Identification of the propulsion phase by the acceleration data. Black circles (●) indicate the start of the push phase and white circles (○) indicate the start of the recovery phase. This means that the period from the black circle to the white circle (the gray-colored area) represents the push phase.

A fourth-order Butterworth bandpass filter (cutoff frequency, 20–450 Hz) was applied to the extracted raw surface EMG data to remove signal noise. Moreover, a linear envelope signal was obtained by full-wave rectification and fourth-order Butterworth low-pass filtering (cutoff frequency, 8 Hz) to smooth out the wavy lines [14]. The filtered surface EMG data of each muscle were normalized based on the maximum value during the 10 cycles and interpolated to 100 points to unify the time among cycles [25].

#### 2.4. Methods of Extracting Muscle Synergies

NMF analysis was performed to extract muscle synergies from the preprocessed surface EMG data [15]. Muscle synergies are expressed by Equation (1):

$$X = W^*H + e \quad (1)$$

$X$  refers to the matrix of the surface EMG data, represented by an  $m \times n$  matrix ( $m$ , number of muscles measured;  $n$ , number of data points). The NMF analysis factorizes  $X$  into muscle weighting ( $W$ ) and activation coefficient ( $H$ ) components and solves the calculation such that  $e$  (the error between  $X$  and  $W^*H$ ) is minimized.  $W$  consists of an  $m \times k$  matrix ( $m$ , number of measured muscles;  $k$ , number of muscle synergies), and  $H$  consists of a  $k \times n$  matrix ( $k$ , number of muscle synergies;  $n$ , number of time data points). In this study, surface EMG data were measured from 10 muscles, and a propulsion cycle was interpolated to 100 points, which means  $m = 10$  and  $n = 100$ .

$k$  was determined based on the variance accounted for ( $VAF$ ). The  $VAF$  is a measure of the reproducibility of the surface EMG data matrix reconstructed from the factorized  $W$  and  $H$  relative to the original matrix  $X$  [26]. It is defined as the coefficient of determination obtained from the uncentered Pearson's correlation coefficient multiplied by 100, which is calculated using the following equation (2):

$$VAF = \left(1 - \frac{\sum_{i=1}^m \sum_{j=1}^n (e_{i,j})^2}{\sum_{i=1}^m \sum_{j=1}^n (E_{i,j})^2}\right) \times 100 \quad (2)$$

where  $i$  indicates the number of muscles ( $1 < i < m = 10$ ) and  $j$  indicates the number of time data points ( $1 < j < n = 100$ ). In this study, two criteria were set: (1) the number of muscle synergies with a  $VAF > 90\%$  and (2) increasing the number of muscle synergies by one, and not increasing the  $VAF$  by  $> 3\%$ . The smallest  $k$  value that satisfied both criteria was adopted [27].

The K-means method, a nonhierarchical clustering analysis, was used to identify muscle synergies common to all participants for muscle weighting ( $W$ ) components extracted by the NMF analysis. The corresponding  $H$  component was extracted for each  $W$  component of the identified muscle synergy, and the mean value was calculated.

### 3. Results

#### 3.1. Kinematic Outcomes

The mean time (mean  $\pm$  standard deviation) required for a 20 m wheelchair propulsion was  $7.5 \pm 0.5$  s (minimum, 6.9 s; maximum, 7.9 s). The average proportion of time that the PP occupied in a wheelchair propulsion cycle was  $44.1 \pm 7.2\%$ .

#### 3.2. Muscle Activity in a Wheelchair Propulsion Cycle

The average activity of each muscle during the wheelchair propulsion cycle is shown in Figure 3. Based on the results of the average proportion of time that the PP occupies in one cycle described above, 0–44% of a wheelchair propulsion cycle was considered the PP, and 44–100% was considered the RP in this study.

The AD, BB, PM, and SA were more active from the beginning of the PP, reaching peak activities at 44%, 41%, 46%, and 53% of the propulsion cycle, respectively. The LD, MD, PD, TB, IS, and UT were highly active in the RP; the LD and PD were active at the beginning of the RP, peaking at 69% and 70% of the propulsion cycle, respectively. The MD, TB, IS, and UT gradually increased from the end of the PP, with the MD at 66%, the TB at 61%, the IS at 68%, and the UT at 71%, showing the highest activity in the RP.

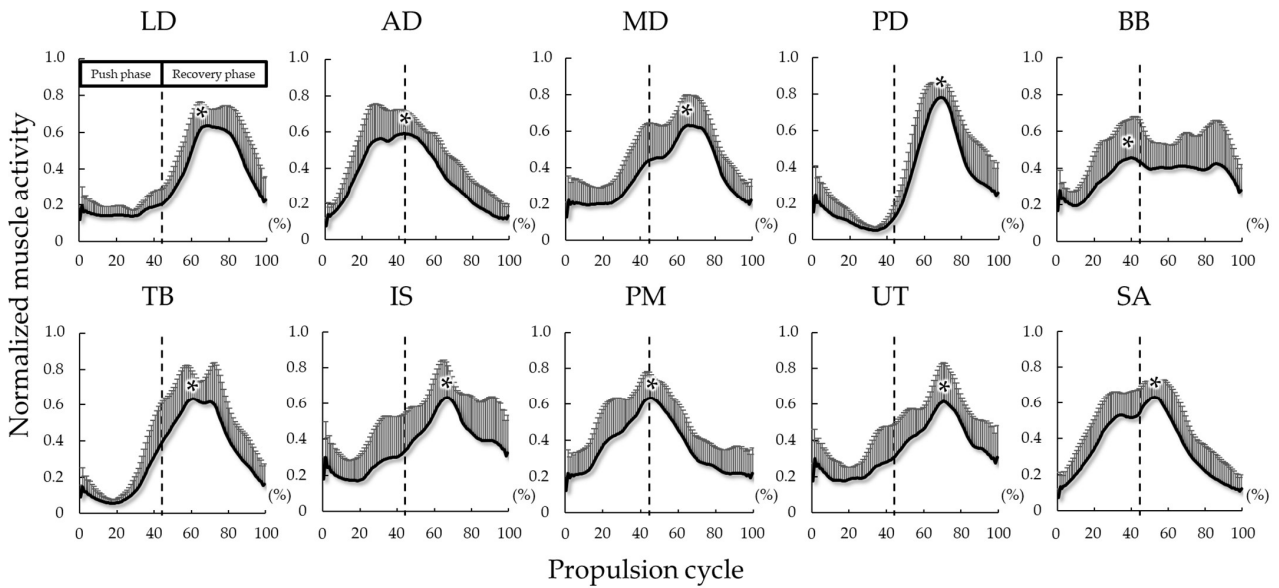


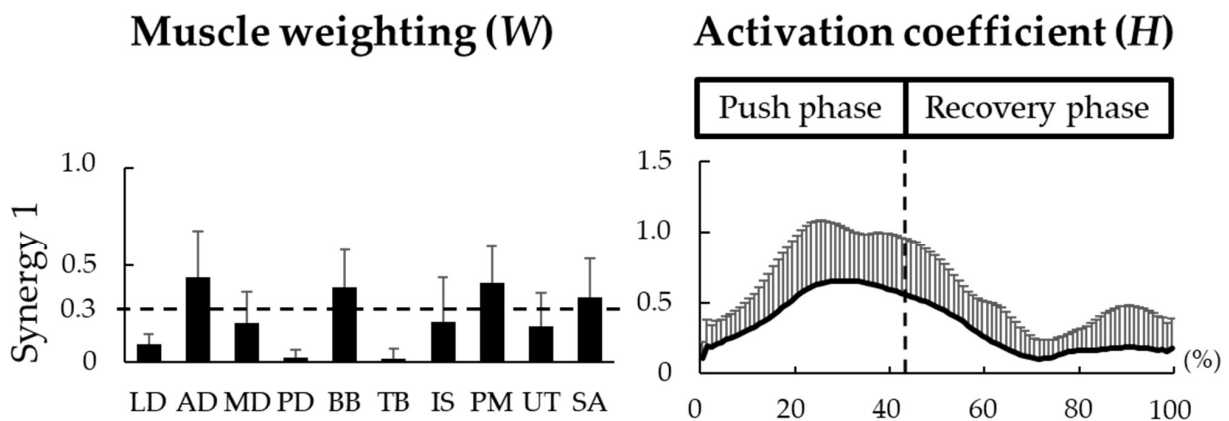
**Figure 3.** The average muscle activity for each muscle during a wheelchair propulsion cycle. These graphs show the activity of each muscle in one propulsion cycle. The vertical dashed line in the graph indicates the timing of the transition from the push phase to the recovery phase (44%), and the asterisk (\*) indicates the point at peak activity. LD, latissimus dorsi; AD, anterior deltoid; MD, middle deltoid; PD, posterior deltoid; BB, biceps brachii; TB, triceps brachii; IS, infraspinatus; PM, pectoralis major; UT, upper trapezius; SA, serratus anterior.

### 3.3. Muscle Synergies in a Wheelchair Propulsion Motion

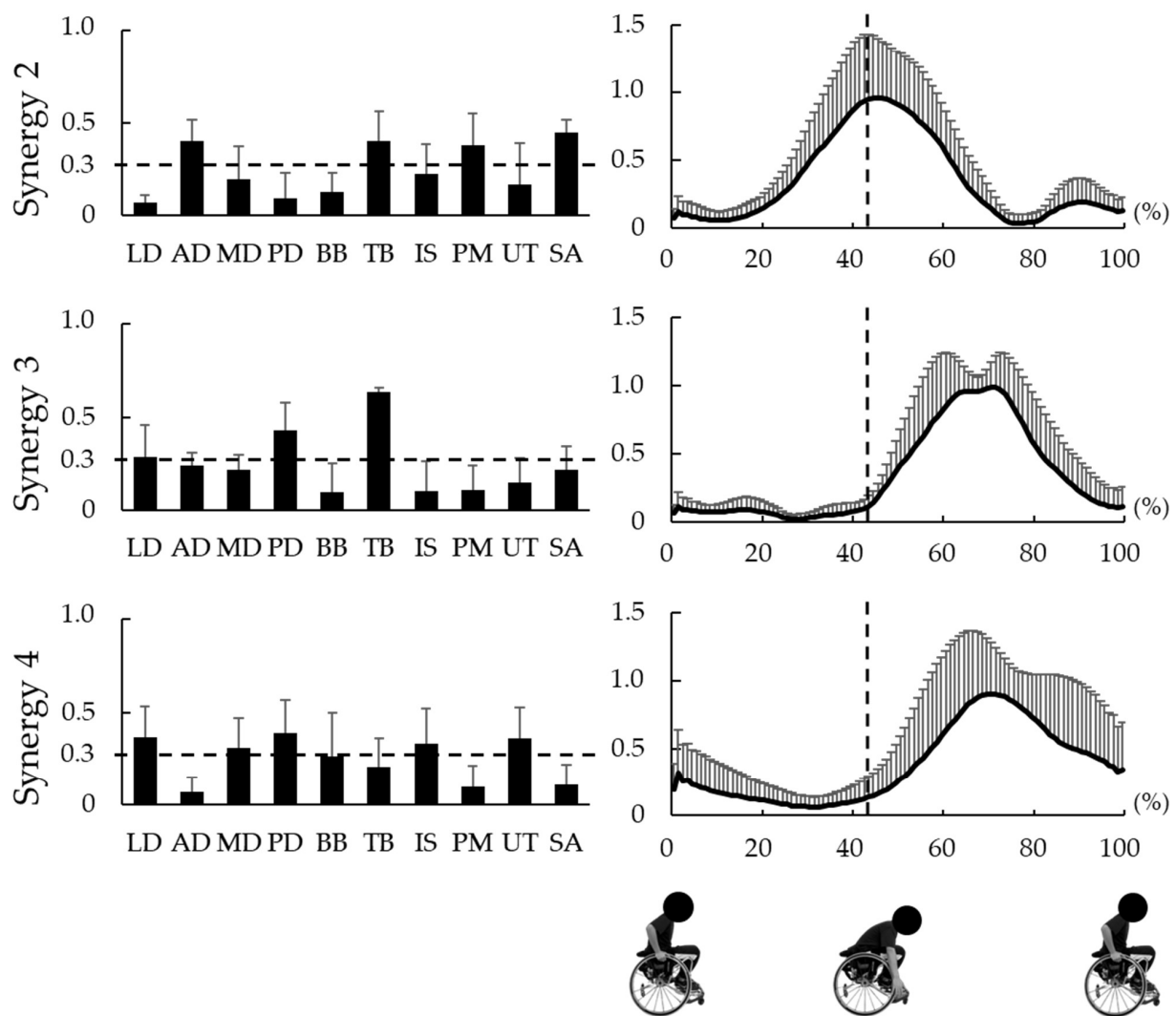
The muscle synergies of all the participants were classified into four categories. In this study, the authors named each synergy from Synergy 1 to Synergy 4 in the order of when the activity reached its peak.

Figure 4 shows the muscle weighting and activation coefficients for each of the four muscle synergies. Synergy 1 began its activity early in the propulsion cycle and reached its peak activity during the PP (32%). In Synergy 1, the muscles with a contribution >0.3 were those that were mainly active in the PP, such as the AD, BB, PM, and SA, which were  $0.44 \pm 0.24$ ,  $0.38 \pm 0.19$ ,  $0.41 \pm 0.19$ , and  $0.33 \pm 0.20$ , respectively.

Synergy 2 was active for approximately 20% of the propulsion cycle, with the highest activity observed during the transition from the PP to the RP (46%). Synergy 2 had a high contribution from the TB, which started its activity at the end of the PP, in addition to the AD, PM, and SA, which showed a high contribution to Synergy 1. Their contributions were  $0.40 \pm 0.12$  for the AD,  $0.41 \pm 0.16$  for the TB,  $0.38 \pm 0.17$  for the PM, and  $0.45 \pm 0.07$  for the SA.



**Figure 4.** Cont.



**Figure 4.** The muscle synergy of wheelchair propulsion. The graph on the right visualizes the contribution of each muscle to the corresponding synergy, where 0.3 or more was considered a muscle with a high contribution. The graph on the left shows the activation timing of each synergy, and the vertical dashed line in the graph indicates the timing of the transition from the push phase to the recovery phase (44%). LD, latissimus dorsi; AD, anterior deltoid; MD, middle deltoid; PD, posterior deltoid; BB, biceps brachii; TB, triceps brachii; IS, infraspinatus; PM, pectoralis major; UT, upper trapezius; SA, serratus anterior.

Synergy 3 was not active in the PP but increased the activity level from the start of the RP, reaching a peak at 70% of the propulsion cycle. Synergy 3 consisted mainly of the PD and TB, among the muscles that showed high activity in the RP. The contributions of the PD and TB to the synergy were  $0.42 \pm 0.15$  and  $0.63 \pm 0.03$ , respectively.

Synergy 4 showed increased activity from the RP, with a peak activity at 71% of the propulsion cycle. Thereafter, the activity gradually decreased but remained active until the beginning of the next PP. In Synergy 4, the LD, MD, PD, IS, and UT, which showed high activity in the RP, contributed  $> 0.3$ , with values of  $0.37 \pm 0.17$ ,  $0.31 \pm 0.16$ ,  $0.39 \pm 0.18$ ,  $0.33 \pm 0.19$ , and  $0.36 \pm 0.17$ , respectively.

#### 4. Discussion

We investigated the muscle synergies of the periarticular shoulder muscles in 12 healthy adult men during the propulsion motion of a wheelchair for WB and found that the motion was performed using four muscle synergies. The results of this study, conducted

on healthy participants, may be useful as standard muscle synergy data during wheelchair propulsion without the influence of disability or pain. Participants had no experience driving a wheelchair for WB, so they practiced for 10 min before the measurement, which may not have been sufficient to familiarize them with the wheelchair propulsion motion.

In this study, the percentage of time that the PP occupied in one cycle was 44%, which is similar to 42% in a previous study that performed motion analysis of wheelchair propulsion motion [24]. Therefore, although this study was conducted with healthy participants who were not accustomed to wheelchair propulsion motion, we proceeded with the discussion based on the assumption that the percentage of time the PP occupied in one wheelchair propulsion cycle was a standard result.

Synergy 1 exhibited the highest activity at 32% of the propulsion cycle, and the contributions of the shoulder flexor muscle groups, including the AD, BB, PM, and SA, were high. In the PP, forward propulsion is achieved primarily by the movement of the shoulder joint from extension to flexion. As the shoulder flexion moment and power are maximal at the PP, the activity of the shoulder flexor muscle group is necessary to generate forward propulsion [28]. That is, Synergy 1 can be thought of as a synergy in which the muscles involved in the shoulder flexion movement coordinate their activities to generate forward propulsion.

Synergy 2 exhibited a peak in activity during the transition from the PP to the RP (46% of the cycle), with high contributions from the AD, TB, PM, and SA. Push muscles were active in the range of 13–58% of the propulsion cycle and continued their activity for a short time after the end of the PP [29]. In the present study, the peak activity of each muscle was also after the end of the PP: 44% in the AD, 46% in the PM, and 53% in the SA. Additionally, muscular exertion during the push is shifted from the elbow flexors to the elbow extensors to generate propulsion [30]. The results of the muscle synergy analysis indicated that the shoulder flexors AD, PM, and SA and the elbow extensor TB contributed to forward propulsion in the latter half of the PP by cooperating with each other.

Synergy 3 exhibited the highest activity of 70% during the propulsion cycle (RP). The LD, MD, PD, TB, IS, and UT activities peaked during the RP, of which Synergy 3 had a higher contribution from shoulder extensors, such as the PD and TB. In the RP, the upper limbs must be moved to the starting position of the next PP by shoulder extensor muscle activity. The results of the muscle synergy analysis showed a low contribution of the LD, which also acts on shoulder joint extension. These results suggest that the participants in this study were dependent on the upper limbs, and their motions were not coordinated with the trunk muscles.

Synergy 4 reached its peak activity at 71% of the cycle (RP), with the LD, MD, PD, IS, and UT contributions  $> 0.3$ . Because the upper limb motion during the RP does not need to follow the hand rim, it is believed that the upper limb joints have a relatively high degree of freedom [31]. However, considering that individuals with shoulder pain have greater kinematic variables in the RP [32], it seems more important to stabilize the joints, including the shoulder girdle. The LD stabilizes the humeral head during shoulder joint extension movements [33], and the MD and PD maintain the afferent position by pressing the humeral head against the glenoid fossa [34]. The IS, one of the rotator cuff muscles, also contributes to the stabilization of the glenohumeral joint [35]. The UT is involved in stabilizing the scapula along with the lower trapezius [36]. From the above, we considered that the LD, MD, PD, IS, and UT are the muscles that stabilize the scapula and glenohumeral joint and that Synergy 4 contributed to the stabilization of the shoulder girdle during the RP.

The findings of this study indicate the presence of four muscle synergies in wheelchair propulsion motion: Synergy 1 reflects propulsion achieved through shoulder flexion and elbow flexion; Synergy 2 involves propulsion through shoulder flexion and elbow extension; Synergy 3 describes the action of shoulder extension returning the upper limb, which has moved forward during the push, back to its original position; and Synergy 4 pertains to the stabilization of the shoulder girdle during the RP. Muscle synergy analysis



allows us to perceive muscles that act simultaneously as a single group rather than being interpreted individually, which may be meaningful because it makes the interpretation of the propulsion motion easier. In the present case, the ten muscles work in coordination with each other to form four groups, and the balance of each muscle activity within a group may be related to injuries and performance. These data can be applied in future studies as foundational information for devising training programs aimed at improving performance and preventing shoulder joint injuries in WB athletes. A previous study reported that in wheelchair propulsion motion, a decrease in PM muscle strength increased AD activity, and a decrease in LD muscle strength increased MD activity [37]. Therefore, WB athletes with impaired trunk movement, such as low pointers, would be expected to alter their muscle synergy patterns by the compensatory activity of the upper limb muscles to offset impaired trunk muscle function. Owing to the higher incidence of shoulder joint injuries in WB athletes who cannot control trunk movements compared with other athletes [38], it is possible that these compensatory changes in muscle synergies are involved in the mechanism of shoulder joint injuries. Further studies are necessary to elucidate the relationship between various muscle synergy patterns and shoulder joint injuries. This study represents the first investigation into the muscle synergy analysis of periarticular shoulder muscles during WB wheelchair propulsion motion, thus serving as the first step toward understanding this relationship.

A limitation of this study was the small sample size and the fact that the participants had no previous experience driving a wheelchair for WB. Because of the lack of familiarity with the propulsion motion, demonstrating the validity and reliability of the muscle synergies extracted in this study remains a topic for future studies. Furthermore, there are limited data on kinematic variables, such as joint angles and moments during wheelchair propulsion motion; therefore, this study was limited to a discussion of muscle activity. If we could clarify the relationship between the muscle synergy patterns and kinematic variables, we could obtain more useful information that would assist in understanding wheelchair propulsion motion.

In the future, we would like to broaden the demographics of the participants to include healthy individuals with wheelchair propulsion experience and WB athletes. This study not only examined the validity and reliability of these results but also investigated the differences in muscle synergy between healthy and WB athletes to contribute to performance improvement and injury prevention in WB athletes.

## 5. Conclusions

We investigated the activity of the periprosthetic shoulder muscles during WB wheelchair propulsion using muscle synergy analysis in healthy adults who had never driven a wheelchair for WB. As a result, four muscle synergies were extracted during motion. Synergies 1 and 2 contributed to the acquisition of forward propulsion during the PP. During the RP, Synergy 3 facilitated the backward movement of the upper limbs, and Synergy 4 contributed to stabilizing the shoulder girdle. This was a preliminary study, and the validity and reliability of the results require further investigation.

**Author Contributions:** Conceptualization, N.M. and Y.U.; methodology, Y.T., M.K. and S.T.; data collection, Y.T., Y.I., S.T. and R.M.; data analyses, Y.T., M.K. and Y.I.; writing—original draft preparation, Y.T.; writing—review and editing, N.M., T.T. and S.A.; supervision, Y.U.; project administration, N.M. All authors have read and agreed to the published version of the manuscript.

**Funding:** This research received no external funding.

**Institutional Review Board Statement:** This study was conducted in accordance with the Declaration of Helsinki and approved by the Ethics Committee for Epidemiology of Hiroshima University (code; E2022-0075, date; 2 August 2022).

**Informed Consent Statement:** Informed consent was obtained from all subjects involved in this study.

**Data Availability Statement:** The raw data supporting the conclusions of this article will be made available by the authors upon request.

**Acknowledgments:** Many thanks to all participants who cooperated in the measurement of this study.

**Conflicts of Interest:** The authors declare no conflicts of interest.

## References

1. IWBF History of Wheelchair Basketball. *IWBF—International Wheelchair Basketball Federation*; IWBF: Mies, Switzerland, 2018; Available online: <https://iwbf.org/the-game/history-wheelchair-basketball/> (accessed on 18 March 2024).
2. Najafabadi, M.G.; Shariat, A.; Anastasio, A.T.; Khah, A.S.; Shaw, I.; Kavianpour, M. Wheelchair basketball, health, competitive analysis, and performance advantage: A review of theory and evidence. *J. Exerc. Rehabil.* **2023**, *19*, 208–218. [[CrossRef](#)]
3. Derman, W.; Runciman, P.; Schweltnus, M.; Jordaan, E.; Blauwet, C.; Webborn, N.; Lexell, J.; van de Vliet, P.; Tuakli-Wosornu, Y.; Kissick, J.; et al. High precompetition injury rate dominates the injury profile at the Rio 2016 Summer Paralympic Games: A prospective cohort study of 51,198 athlete days. *Br. J. Sports Med.* **2018**, *52*, 24–31. [[CrossRef](#)]
4. Sá, K.; Costa e Silva, A.; Gorla, J.; Silva, A.; Magno e Silva, M. Injuries in wheelchair basketball players: A systematic review. *Int. J. Environ. Res. Public Health* **2022**, *19*, 5869. [[CrossRef](#)]
5. Akbar, M.; Brunner, M.; Ewerbeck, V.; Wiedenhöfer, B.; Grieser, T.; Bruckner, T.; Loew, M.; Raiss, P. Do overhead sports increase risk for rotator cuff tears in wheelchair users? *Arch. Phys. Med. Rehabil.* **2015**, *96*, 484–488. [[CrossRef](#)]
6. Lin, D.J.; Wong, T.T.; Kazam, J.K. Shoulder Injuries in the Overhead-Throwing Athlete: Epidemiology, Mechanisms of Injury, and Imaging Findings. *Radiology* **2018**, *286*, 370–387. [[CrossRef](#)]
7. Karasuyama, M.; Oike, T.; Okamatsu, S.; Kawakami, J. Shoulder pain in wheelchair basketball athletes: A scoping review. *J. Spinal Cord. Med.* **2023**, *46*, 753–759. [[CrossRef](#)]
8. Tsunoda, K.; Mutsuzaki, H.; Kanae, K.; Tachibana, K.; Shimizu, Y.; Wadano, Y. Associations between wheelchair user’s shoulder pain index and tendinitis in the long head of the biceps tendon among female wheelchair basketball players from the Japanese national team. *Asia Pac. J. Sports Med. Arthrosc. Rehabil. Technol.* **2021**, *24*, 29–34. [[CrossRef](#)]
9. de Freitas, G.R.; Abou, L.; de Lima, A.; Rice, L.A.; Ilha, J. Measurement properties of clinical instruments for assessing manual wheelchair mobility in individuals with spinal cord injury: Systematic review. *Arch. Phys. Med. Rehabil.* **2023**, *104*, 656–672. [[CrossRef](#)]
10. Vanlandewijck, Y.; Theisen, D.; Daly, D. Wheelchair propulsion biomechanics: Implications for wheelchair sports. *Sports Med.* **2001**, *31*, 339–367. [[CrossRef](#)]
11. Qi, L.; Guan, S.; Zhang, L.; Liu, H.L.; Sun, C.K.; Ferguson-Pell, M. The effect of fatigue on wheelchair users’ upper limb muscle coordination patterns in time-frequency and principal component analysis. *IEEE Trans. Neural Syst. Rehabil. Eng.* **2021**, *29*, 2096–2102. [[CrossRef](#)]
12. Lacquaniti, F.; Ivanenko, Y.P.; Zago, M. Patterned control of human locomotion. *J. Physiol.* **2012**, *590*, 2189–2199. [[CrossRef](#)]
13. Cheung, V.C.; d’Avella, A.; Tresch, M.C.; Bizzi, E. Central and sensory contributions to the activation and organization of muscle synergies during natural motor behaviors. *J. Neurosci.* **2005**, *25*, 6419–6434. [[CrossRef](#)]
14. Matsuura, Y.; Matsunaga, N.; Akuzawa, H.; Oshikawa, T.; Kaneoka, K. Comparison of muscle coordination during front crawl and backstroke with and without swimmer’s shoulder pain. *Sports Health* **2024**, *16*, 89–96. [[CrossRef](#)]
15. Lee, D.D.; Seung, H.S. Learning the parts of objects by non-negative matrix factorization. *Nature* **1999**, *401*, 788–791. [[CrossRef](#)]
16. Jie, T.; Xu, D.; Zhang, Z.; Teo, E.C.; Baker, J.S.; Zhou, H.; Gu, Y. Structural and Organizational Strategies of Locomotor Modules during Landing in Patients with Chronic Ankle Instability. *Bioengineering* **2024**, *11*, 518. [[CrossRef](#)]
17. Baifa, Z.; Xinglong, Z.; Dongmei, L. Muscle coordination during archery shooting: A comparison of archers with different skill levels. *Eur. J. Sport Sci.* **2023**, *23*, 54–61. [[CrossRef](#)]
18. Matsuura, Y.; Matsunaga, N.; Akuzawa, H.; Kojima, T.; Oshikawa, T.; Iizuka, S.; Okuno, K.; Kaneoka, K. Difference in muscle synergies of the butterfly technique with and without swimmer’s shoulder. *Sci. Rep.* **2022**, *12*, 14546. [[CrossRef](#)]
19. Medola, F.O.; Elui, V.M.; da Santana, C.S.; Fortulan, C.A. Aspects of manual wheelchair configuration affecting mobility: A review. *J. Phys. Ther. Sci.* **2014**, *26*, 313–318. [[CrossRef](#)]
20. Soltau, S.L.; Slowik, J.S.; Requejo, P.S.; Mulroy, S.J.; Neptune, R.R. An investigation of bilateral symmetry during manual wheelchair propulsion. *Front. Bioeng. Biotechnol.* **2015**, *3*, 86. [[CrossRef](#)]
21. Hermens, H.J.; Freriks, B.; Merletti, R.; Stegeman, D.; Blok, J.; Rau, G.; Disselhorst-Klug, C.; Hägg, G. *SENIAM European Recommendations for Surface Electromyography: Results of the SENIAM Project*; Roessingh Research and Development: Enschede, The Netherlands, 1999.
22. Ribeiro, D.C.; Sole, G.; Venkat, R.; Shemmell, J. Differences between clinician- and self-administered shoulder sustained mobilization on scapular and shoulder muscle activity during shoulder abduction: A repeated-measures study on asymptomatic individuals. *Musculoskelet. Sci. Pract.* **2017**, *30*, 25–33. [[CrossRef](#)]
23. Bergamini, E.; Morelli, F.; Marchetti, F.; Vannozzi, G.; Polidori, L.; Paradisi, F.; Traballes, M.; Cappozzo, A.; Delussu, A.S. Wheelchair propulsion biomechanics in junior basketball players: A method for the evaluation of the efficacy of a specific training program. *Biomed. Res. Int.* **2015**, *2015*, 275965. [[CrossRef](#)]

24. Cavallone, P.; Vieira, T.; Quaglia, G.; Gazzoni, M. Electromyographic activities of shoulder muscles during Handwheelchair.Q. vs pushrim wheelchair propulsion. *Med. Eng. Phys.* **2022**, *106*, 103833. [[CrossRef](#)]
25. Turpin, N.A.; Uriac, S.; Dalleau, G. How to improve the muscle synergy analysis methodology? *Eur. J. Appl. Physiol.* **2021**, *121*, 1009–1025. [[CrossRef](#)]
26. Tresch, M.C.; Cheung, V.C.; d’Avella, A. Matrix factorization algorithms for the identification of muscle synergies: Evaluation on simulated and experimental data sets. *J. Neurophysiol.* **2006**, *95*, 2199–2212. [[CrossRef](#)]
27. Cheung, V.C.; Piron, L.; Agostini, M.; Silvoni, S.; Turolla, A.; Bizzi, E. Stability of muscle synergies for voluntary actions after cortical stroke in humans. *Proc. Natl. Acad. Sci. USA* **2009**, *106*, 19563–19568. [[CrossRef](#)]
28. Morrow, M.M.; Hurd, W.J.; Kaufman, K.R.; An, K.N. Shoulder demands in manual wheelchair users across a spectrum of activities. *J. Electromyogr. Kinesiol.* **2010**, *20*, 61–67. [[CrossRef](#)]
29. Mulroy, S.J.; Farrokhi, S.; Newsam, C.J.; Perry, J. Effects of spinal cord injury level on the activity of shoulder muscles during wheelchair propulsion: An electromyographic study. *Arch. Phys. Med. Rehabil.* **2004**, *85*, 925–934. [[CrossRef](#)]
30. Bregman, D.J.; van Drongelen, S.; Veeger, H.E. Is effective force application in handrim wheelchair propulsion also efficient? *Clin. Biomech.* **2009**, *24*, 13–19. [[CrossRef](#)]
31. Jayaraman, C.; Moon, Y.; Rice, I.M.; Hsiao Weckslar, E.T.; Beck, C.L.; Sosnoff, J.J. Shoulder pain and cycle to cycle kinematic spatial variability during recovery phase in manual wheelchair users: A pilot investigation. *PLoS ONE* **2014**, *9*, e89794. [[CrossRef](#)]
32. de Groot, S.; Veeger, H.E.; Hollander, A.P.; van der Woude, L.H. Short-term adaptations in co-ordination during the initial phase of learning manual wheelchair propulsion. *J. Electromyogr. Kinesiol.* **2003**, *13*, 217–228. [[CrossRef](#)]
33. Escamilla, R.F.; Andrews, J.R. Shoulder muscle recruitment patterns and related biomechanics during upper extremity sports. *Sports Med.* **2009**, *39*, 569–590. [[CrossRef](#)] [[PubMed](#)]
34. Moser, T.; Lecours, J.; Michaud, J.; Bureau, N.J.; Guillin, R.; Cardinal, É. The deltoid, a forgotten muscle of the shoulder. *Skelet. Radiol.* **2013**, *42*, 1361–1375. [[CrossRef](#)] [[PubMed](#)]
35. Lin, H.T.; Su, F.C.; Wu, H.W.; An, K.N. Muscle forces analysis in the shoulder mechanism during wheelchair propulsion. *Proc. Inst. Mech. Eng. H* **2004**, *218*, 213–221. [[CrossRef](#)] [[PubMed](#)]
36. Camargo, P.R.; Neumann, D.A. Kinesiologic considerations for targeting activation of scapulothoracic muscles—Part 2: Trapezius. *Braz. J. Phys. Ther.* **2019**, *23*, 467–475. [[CrossRef](#)]
37. Slowik, J.S.; McNitt-Gray, J.L.; Requejo, P.S.; Mulroy, S.J.; Neptune, R.R. Compensatory strategies during manual wheelchair propulsion in response to weakness in individual muscle groups: A simulation study. *Clin. Biomech.* **2016**, *33*, 34–41. [[CrossRef](#)]
38. Yildirim, N.U.; Comert, E.; Ozengin, N. Shoulder pain: A comparison of wheelchair basketball players with trunk control and without trunk control. *J. Back. Musculoskelet. Rehabil.* **2010**, *23*, 55–61. [[CrossRef](#)]

**Disclaimer/Publisher’s Note:** The statements, opinions and data contained in all publications are solely those of the individual author(s) and contributor(s) and not of MDPI and/or the editor(s). MDPI and/or the editor(s) disclaim responsibility for any injury to people or property resulting from any ideas, methods, instructions or products referred to in the content.